Surface-Enhanced Optical Third-Harmonic Generation in Ag Island Films

E. M. Kim, S. S. Elovikov, T. V. Murzina, A. A. Nikulin, and O. A. Aktsipetrov*

Department of Physics, Moscow State University, 119992 Moscow, Russia

M. A. Bader and G. Marowsky

Laser-Laboratorium Göttingen, D-37077 Göttingen, Germany
(Received 18 May 2005; published 23 November 2005)

Surface-enhanced optical third-harmonic generation (THG) is observed in silver island films. The THG intensity from Ag nanoparticles is enhanced by more than 2 orders of magnitude with respect to the THG intensity from a smooth and homogeneous silver surface. This enhancement is attributed to a local plasmon excitation and resonance of the local field at the third-harmonic wavelength. The diffuse and depolarized component of the enhanced THG is associated with the third-order hyper-Rayleigh scattering in a two-dimensional random array of silver nanoparticles.

Observation of surface-enhanced nonlinear-optical effects in silver island films dates back to two 1981 papers by Wokaun *et al.* [1,2], where surface-enhanced optical second-harmonic generation (SHG) and surface-enhanced Raman scattering (SERS) were observed in silver island films. The enhancement of the SHG intensity by up to 3 orders of magnitude was attributed in Ref. [1] to the resonant enhancement of the local field at the second-harmonic (SH) wavelength, mediated by the excitation of the local surface plasmons in silver nanoparticles. This plasmon mechanism of the local field enhancement, introduced by Berreman [3] and Moskovits [4], was intensively discussed in the context of SERS active structures and surface-enhanced SHG from electrochemically roughened silver surfaces [5] and rough surfaces of other metals [6]. According to this approach, nonlinear polarization of a rough metal surface or an array of small metal particles is given by $P_{2\omega} = L_{2\omega}\chi^{(2)}(2\omega)L_\omega^2 E_\omega^2$ at the SH wavelength and $P_{3\omega} = L_{3\omega}\chi^{(3)}(3\omega)L_\omega^3 E_\omega^3$ at the third-harmonic (TH) wavelength, where $\chi^{(2)}(2\omega)$ and $\chi^{(3)}(3\omega)$ are the second- and third-order susceptibilities of the metal, respectively; E_ω is the optical field at fundamental wavelength; and L_ω, $L_{2\omega}$, and $L_{3\omega}$ are the local field factors at the corresponding wavelengths.

The spectral dependence of the local field factor of an array of small metal spheroids embedded in a dielectric matrix within the simple approach in dipole and effective media approximations is given by [7]:

$$L(\lambda) = \frac{\varepsilon_d(\lambda)}{\varepsilon_d(\lambda) + [\varepsilon_m(\lambda) - \varepsilon_d(\lambda)](N - q/3)}, \quad (1)$$

where $\varepsilon_d(\lambda)$ and $\varepsilon_m(\lambda)$ are the dielectric constants of the dielectric matrix and of the metal, respectively; N is the shape-dependent depolarization factor of the spheroids; and q is the filling factor, i.e., the relative fraction of the metal in a composite material. The resonant wavelength of the local field factor λ_{res} corresponds to setting the real part

of the denominator in Eq. (1) to zero: $\mathrm{Re}[\varepsilon_d(\lambda_{res}) + [\varepsilon_m(\lambda_{res}) - \varepsilon_d(\lambda_{res})](N - q/3)] = 0$. For an isolated small Ag sphere in vacuum, $\lambda_{res} \approx 200$ nm. Three factors result in the redshift of λ_{res} up to the visible range for an array of particles: (1) the distortion of the particle shape, (2) the dipole-dipole interaction between particles, and (3) an increase in the dielectric constant of the matrix material. The resonant increase of the local field factor at λ_{res} results in a manyfold increase of the nonlinear-optical response from a nanoparticle array.

Up to the present time, the experimental studies of local plasmon enhancement in island films were restricted to SERS and SHG. Figure 1(d), taken from Ref. [1], shows the dependencies of the local field factor in Ag island films on the mass thickness, $d_M = m/\rho$, where m is the mass of metal deposited per unit area and ρ is the bulk density of Ag. These dependencies show a maxima at $d_M \approx 2.0$ nm and $d_M \approx 6.0$ nm for wavelengths of 532 and 1064 nm, respectively. The decrease of d_M results in the blueshift of λ_{res} due to a decrease of the interparticle interaction. One might anticipate that the resonance at the THG wavelength $\lambda_{res} = 355$ nm for the 1064 nm fundamental wavelength can be attained for $d_M \approx 1$ nm.

Another peculiarity of the surface-enhanced SHG from metal island films is the diffuseness of the SH radiation [5,6]. This is a manifestation of the second-order hyper-Rayleigh scattering. Silver island films are random arrays of nanoparticles characterized by random spatial inhomogeneity of nonlinear susceptibilities [8] and local field factors [9]. This inhomogeneity is the source of the diffuse SHG radiation in the hyper-Rayleigh scattering.

The enhancement and diffuseness observed, up to now, for SHG are general features of the nonlinear-optical effects in island films and are expected to be observed in THG. Meanwhile, in spite of this analogy, there is a principal difference between SHG and THG in metal nanoparticles: $\chi^{(2)}$ is localized at the surface of nanoparticles and vanishes in the bulk of a centrosymmetric metal,
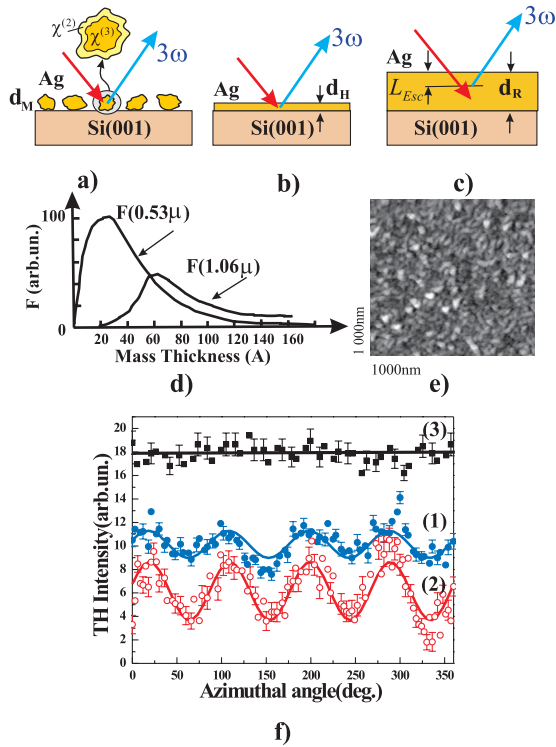
FIG. 1 (color).   Schematics of (a) a silver island film with a
mass thickness of d_M [inset in (a) shows the localization of $\chi^{(2)}$
and $\chi^{(3)}$ in nanoparticles]; (b) a model homogeneous film of the
equivalent thickness of $d_H \equiv d_M$; (c) a thick homogeneous
reference Ag film with a thickness of d_R and an escape depth
of L_{Esc} for the TH wave; (d) dependencies of the local field
factors at wavelengths of 1.064 and 0.532 μm on the mass
thickness (from Ref. [1]); (e) the AFM image of silver island
film; (f) the THG intensity as a function of the azimuthal angle
from: (1) a silver island film with $d_M \approx 1$ nm on a Si(001)
substrate, (2) a silver-free Si(001) substrate, (3) a thick homoge-
neous reference Ag film with a thickness of $d_R \approx 40$ nm; the
solid lines are results of approximations.

whereas $\chi^{(3)}$ is a bulk localized nonlinearity [10], as shown
schematically in the inset in Fig. 1(a).

This difference in localization of nonlinearities results in
a major qualitative difference between plasmon-assisted
SHG and THG in arrays of metal nanoparticles. $\chi^{(3)}(r)$ as
the function of the interparticle coordinate r possesses the
same sign for the whole particle, whereas $\chi^{(2)}(r)$ has a
different sign at the opposite sides of particle: The sign of
the surface $\chi^{(2)}(r)$ of centrosymmetric materials depends
on the direction of the normal to the particle surface. This
results in different mechanisms of reradiation of nonlinear
signal: The THG signal is radiated constructively by the
whole nanoparticle, whereas the SHG fields from the op-
posite sides of the nanoparticle surface interfere destruc-
tively, which drastically suppresses an outgoing SHG
signal. Another consequence of the nonlinearity localiza-
tion is the difference in the second- and third-order hyper-
Rayleigh scattering. The second-order hyper-Rayleigh

scattering is attributed to the random inhomogeneity of
particle surface nonlinearity and spatial fluctuations of
local field factors in the surface region, whereas the
third-order hyper-Rayleigh scattering is attributed to the
random inhomogeneity of the bulk nonlinearity and the
corresponding spatial fluctuations of the local field factors.
This implies that morphological information that can be
obtained for nanoparticle arrays from nonlinear-optical
probes is different for the plasmon-assisted SHG and THG.

In this Letter, surface-enhanced THG and third-order
hyper-Rayleigh scattering are observed in Ag island films.
The resonant plasmon mechanism of the THG enhance-
ment is proved.

The films were prepared by thermal evaporation of silver
onto the substrates of silicon Si(001) wafers at a rate of
3–4 Å/s and residual pressure of 10^{-5} Torr. The silicon
wafers were chosen as substrates because of the flatness
and homogeneity of the surface and the simplicity of the
chemical etching procedure that was used for the prepara-
tion of a steplike SiO_2 wedge [see the scheme in Fig. 2(b)].
Three types of Ag films are studied: a Ag island film with a
mass thickness of $d_M \approx 1$ nm and expected plasmon reso-
nance at $\lambda_{\mathrm{res}} \sim 355$ nm, a Ag island film with plasmon
resonance in the vicinity of $\lambda_{\mathrm{res}} \sim 270$ nm on the silicon
oxide steplike wedge, and a thick homogeneous Ag refer-
ence film with a thickness of $d_R \approx 40$ nm. The thick
homogeneous Ag film was used as a reference source of
the nonenhaced bulk THG for the measurement of the
THG enhancement from island films. An atomic force
microscope (AFM), in the constant force mode, and with
a height resolution of 1 nm and lateral resolution of ap-
proximately 10 nm, was used to characterize the morphol-
ogy of the samples. Figure 1(e) shows the AFM image of a
Ag island film. A cross section of the profile shows that the
average lateral size and height of silver nanoparticles are
about 40 and 3 nm, respectively.

The outputs of two laser systems are used as the fun-
damental radiation in the THG and SHG experiments:
(1) an optical parametric oscillator (OPO) laser system,
"Spectra-Physics 710," with a wavelength that is tunable
in the spectral range from 490 to 680 nm, a pulse duration
of 4 ns, and a pulse intensity of 2 MW/cm^2; and (2) a
Q-switched YAG:Nd^{3+} laser with a wavelength of
1064 nm, a pulse duration of 15 ns, and a pulse intensity
of about 1 MW/cm^2. The TH (SH) radiation was filtered
out by appropriate UV and blue-green color and bandpass
filters and detected by a photomultiplier tube and gated
electronics. To normalize the THG (SHG) intensity by the
OPO and YAG:Nd^{3+} laser fluency, and the spectral sensi-
tivity of the optical detection system, a reference channel
was used with a Z-cut quartz plate as a nonlinear-optical
reference and with a detection system identical to that of
the "sample" channel. Polar rotation of the detector sys-
tem enables us to measure the linear Rayleigh scattering
pattern and the THG and SHG scattering patterns [see
Fig. 2(a)].
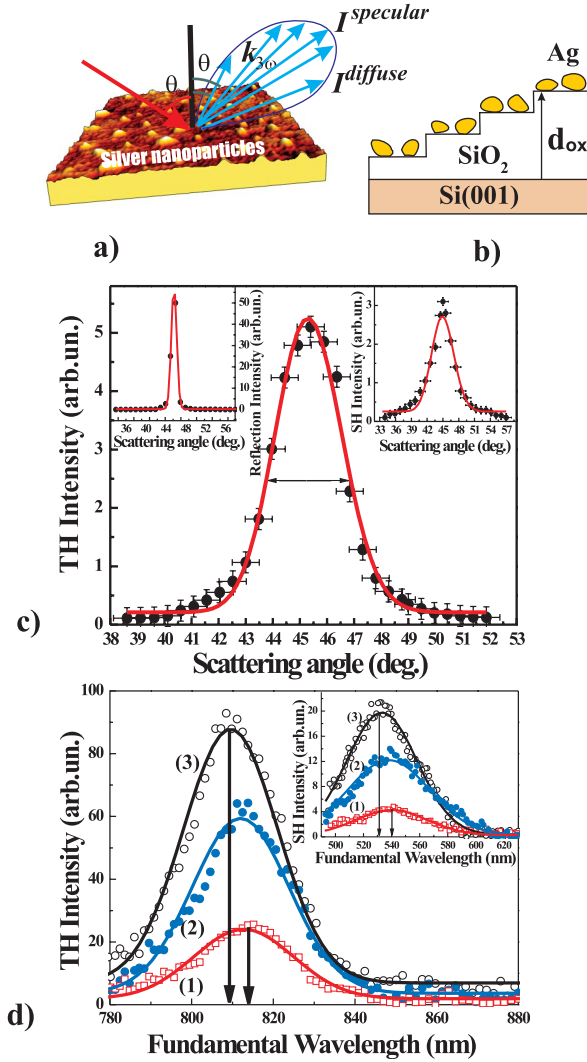
FIG. 2 (color).   (a) The scheme of the hyper-Rayleigh scattering experiment; (b) scheme of silicon oxide steplike wedge as a variable spacer between the island film and the high-dielectric constant material (silicon); d_{ox} is the thickness of the silicon oxide steps; (c) THG scattering pattern: the THG intensity from the island film as a function of polar scattering angle (angular width is $3° \pm 0.5°$); left inset is the linear Rayleigh scattering pattern, with angular width of $1° \pm 0.5°$; right inset is the SHG scattering pattern, with angular width of $5° \pm 0.5°$; solid lines are approximations with Eq. (3); (d) main panel: dependencies of the THG intensity on the fundamental wavelength for Ag island films deposited on the SiO$_2$ steplike wedge for $d_{ox} = 2$ (1), 70 (2), and 100 nm (3); inset: the same for the SHG intensity spectra; solid lines are approximations by Gaussian function.

In order to observe and measure an enhancement in THG, two experimental points have to be taken into account: (1) the THG signal from Ag island film should be distinguished from the Si(001) substrate contribution, and (2) the THG intensity should be integrated over the diffuse THG scattering pattern. The following paragraphs focus on these points.

The curve (1) in Fig. 1(f) shows the azimuthal dependence of the THG intensity from the sample of a Ag island film in the specular direction for the s-in, s-out combination of polarizations of the fundamental and TH waves. The anisotropic component of the THG signal is related to the nonlinear response of the Si(001) substrate, whereas the isotropic THG is attributed to both Ag nanoparticles and the Si substrate. To distinguish the THG contribution of the Ag island film from that of the substrate, the azimuthal dependence of the THG intensity from Si(001) is measured in the same s-in, s-out geometry [curve (2) in Fig. 1(f)]. The ratio of the anisotropic components of THG from silver island film on Si(001), $I_{IF+Si}^{anis}(3\omega)$, and silver-free Si(001) substrate, $I_{Si}^{anis}(3\omega)$, gives an attenuation coefficient of the THG response from the substrate due to the absorption and scattering in the silver coverage: $\alpha_{3\omega} = I_{IF+Si}^{anis}(3\omega)/I_{Si}^{anis}(3\omega) = 0.46$. The estimation of the $\alpha_{3\omega}$ coefficient is the first step in the determination of the THG enhancement for Ag island films. The relative value of the THG intensity from Ag nanoparticles in the specular direction is $I_{IF}^{spec}(3\omega) = I_{IF+Si}^{is}(3\omega) - \alpha_{3\omega}I_{Si}^{is}(3\omega)$, where $I_{IF+Si}^{is}(3\omega)$ and $I_{Si}^{is}(3\omega)$ are the isotropic components of THG from the island film on Si(001) and from a silver-free substrate, respectively. Obtaining the total intensity of the diffuse THG from Ag nanoparticles is the second step in the determination of the THG enhancement. This demands the measurement of the THG scattering pattern, which is dependent on the diffuse THG intensity, which in turn depends on the polar scattering angle: $I_{IF}(3\omega, \theta) = I_{IF}^{spec}(3\omega)S_{3\omega}(\theta)$, where θ and $S_{3\omega}(\theta)$ are the polar scattering angle and the normalized form factor of the third-order hyper-Rayleigh scattering, respectively. The main panel in Fig. 2(c) shows the experimental scattering pattern of the diffuse THG from silver island films where the angular width of the normalized form factor is approximately $3° \pm 0.5°$. This sufficiently exceeds the angular width of $1° \pm 0.5°$ of the scattering pattern of the linear Rayleigh scattering from the same silver island film presented in the left inset in Fig. 2(c), whereas the angular width of the SHG scattering pattern is approximately $5° \pm 0.5°$. The total intensity of the diffuse THG can be obtained by angular integration of the THG scattering pattern and, in the case of the small angular width of $S_{3\omega}(\theta)$, is given by: $I_{IF}(3\omega) = I_{IF}^{spec}(3\omega)[\frac{1}{\Omega}\int_{\Delta\theta}S_{3\omega}(\theta)d\theta]^2 \approx 0.6 \times 10^2 I_{IF}^{spec}(3\omega)$, where Ω is the angular aperture of the THG detection system and $\Delta\theta$ is the angular interval of integration. To estimate quantitatively the THG enhancement, we consider the total THG intensity of the specular THG from a model homogeneous film with an equivalent thickness of $d_H = 1$ nm and compare this with the THG intensity from a thick homogeneous reference film with a thickness of $d_R \approx 40$ nm [see Figs. 1(b) and 1(c)]. The THG intensity detected from the reference film comes from the Ag layer corresponding to the escape depth L_{Esc} of the TH wave [curve (3) in Fig. 1(f)]. In our experimental conditions,

$L_{\text{Esc}} \sim 7$ nm for $\lambda_{3\omega} = 355$ nm. Thus, the enhancement of the THG intensity from Ag island film with respect to a thick homogeneous Ag film is given by:

$$G = \frac{I_{\text{IF}}(3\omega)}{I_{\text{HF}}(3\omega)} \approx \frac{I_{\text{IF}}(3\omega)}{I_{\text{Ref}}(3\omega)} \left[\frac{L_{\text{Esc}}}{d_H}\right]^2 \approx 1.2 \times 10^2, \quad (2)$$

where $I_{\text{HF}}(3\omega)$ and $I_{\text{Ref}}(3\omega)$ are the THG intensity from the model homogeneous film with the thickness of $d_H \equiv d_M$ and the thick homogeneous reference Ag film, respectively. To prove the plasmon assistance in the THG enhancement, the dependencies of the THG intensity on the fundamental wavelength are studied for Ag island films deposited onto a steplike SiO_2 wedge on a silicon wafer. Silicon oxide steps serve as variable spacers between the silver nanoparticles and the silicon substrate, which is a high-dielectric constant material. Variations of SiO_2 thickness, d_{ox}, result in the variations of the effective dielectric constant $\varepsilon_{dl}(d_{ox}) = \varepsilon'_{dl}(d_{ox}) + i\varepsilon''_{dl}(d_{ox})$ in Eq. (1): The increase of d_{ox} corresponds to the decrease of the effective $\varepsilon_{dl}(d_{ox})$. Theoretical modeling [11] shows that the decrease of the real part, $\varepsilon'_{dl}(d_{ox})$, results in the blueshift of the resonant plasmon wavelength, whereas the decrease of the imaginary part, $\varepsilon''_{dl}(d_{ox})$, leads to the enhancement of the local field amplitude.

The main panel in Fig. 2(d) shows a set of THG spectra for d_{ox} increasing in the range from 2 to 100 nm. The observed effects of d_{ox} on the THG spectra as SiO_2 thickness increases from 2 to 100 nm is twofold: (1) An apparent blueshift of approximately 6 nm of the THG resonance and (2) a more than fourfold increase of the THG resonant intensity. These changes correspond to the decrease of the effective dielectric constant of Ag islands situated at different steps of the SiO_2 wedge. An analogous blueshift of about 10 nm and manyfold increase of the resonant SHG intensity are observed in the same conditions [refer to the inset in Fig. 2(d)]. The impact of the dielectric constant of the substrate on the resonant properties of the surface-enhanced THG and SHG proves the plasmon-assisted mechanism of the enhancement. A slight difference in the spectral shift for THG and SHG can be associated with the different localizations of $\chi^{(3)}$ and $\chi^{(2)}$ in metal nanoparticles. Moreover, different spatial localizations of nonlinear susceptibilities in metal particles can result in different parameters of scattering patterns at the TH and SH wavelengths from a random array of Ag nanoparticles. Normalized form factors at the TH and SH wavelengths are given by:

$$S_{3\omega,2\omega}(\theta) \sim \exp[-M_{3\omega,2\omega}k^2_{3\omega,2\omega}l^2_{\text{cor}}(3\omega, 2\omega)], \quad (3)$$

where $l_{\text{cor}}(3\omega, 2\omega)$ is the correlation length at the TH and SH wavelengths, respectively, $k_{3\omega,2\omega} = 2\pi(\sin\theta - \sin\theta_0)/\lambda_{3\omega,2\omega}$, and $M_{3\omega,2\omega}$ is an adjustable parameter at

the TH and SH wavelengths, respectively, and θ_0 is the angle of incidence. The approximation of the diffuse THG and SHG scattering patterns [Fig. 2(c), solid lines] by Eq. (3) corresponds to the correlation lengths of $l_{\text{cor}}(3\omega) \approx 42$ nm and $l_{\text{cor}}(2\omega) \approx 20$ nm. The former probably corresponds to the average Ag particle size of 40 nm obtained from the AFM measurements because of the bulk localization of $\chi^{(3)}$. Meanwhile, the latter, being twice as small as $l_{\text{cor}}(3\omega)$, corresponds to the smaller scale of the $\chi^{(2)}$ inhomogeneity due to its surface localization within the individual particles.

In conclusion, surface-enhanced THG is observed in Ag island films with an enhancement of 1.2×10^2, which is attributed to the local surface plasmon excitation in Ag nanoparticles at the TH wavelength. Diffuseness of the surface-enhanced THG allows us to associate this effect with the third-order hyper-Rayleigh scattering in a random array of nanoparticles. The difference in scattering patterns and spectroscopic resonances between the surface-enhanced THG and SHG can be attributed to the different localizations of $\chi^{(3)}$ and $\chi^{(2)}$ in nanoparticles.

*Electronic address: aktsip@shg.ru

[1] A. Wokaun, J. G. Bergman, J. P. Heritage, A. M. Glass, P. F. Liao, and D. H. Olson, Phys. Rev. B **24**, 849 (1981).
[2] A. Wokaun, J. P. Gordon, and P. F. Liao, Phys. Rev. Lett. **48**, 957 (1982).
[3] D. W. Berreman, Phys. Rev. **163**, 855 (1967).
[4] M. Moskovits, J. Chem. Phys. **69**, 4159 (1978).
[5] C. K. Chen, A. R. B. de Castro, and Y. R. Shen, Phys. Rev. Lett. **46**, 145 (1981).
[6] G. T. Boyd, Th. Rasing, J. R. R. Leite, and Y. R. Shen, Phys. Rev. B **30**, 519 (1984).
[7] V. I. Emelyanov and N. I. Koroteev, Sov. Phys. Usp. **135**, 345 (1981).
[8] O. A. Aktsipetrov, P. V. Elyutin, A. A. Nikulin, and E. A. Ostrovskaya, Phys. Rev. B **51**, 17 591 (1995).
[9] M. Breit, V. A. Podolsky, S. Gresillon, G. von Plessen, J. Feldman, J. C. Rivoal, P. Gadenne, A. K. Sarychev, and V. M. Shalaev, Phys. Rev. B **64**, 125106 (2001).
[10] N. Bloembergen, R. K. Chang, S. S. Jha, and C. H. Lee, Phys. Rev. **174**, 813 (1968).
[11] O. A. Aktsipetrov, E. M. Dubinina, S. S. Elovikov, E. D. Mishina, A. A. Nikulin, N. N. Novikova, and M. S. Strebkov, Solid State Commun. **70**, 1021 (1989).